Theoretical Study of the Thermal Decomposition Pathways of 2-H Heptafluoropropane

Shane D. Peterson and Joseph S. Francisco*

Department of Chemistry and Department of Earth and Atmospheric Sciences, Purdue University, West Lafayette, Indiana 47907

Received: July 17, 2001; In Final Form: November 12, 2001

The structures, vibrational frequencies, and energetics of 2-H heptafluoropropane (CF_3CHFCF_3) as well as the thermal decomposition products and transition-state molecules have been studied theoretically with both ab initio and density functional methods. Of a total of 12 primary reaction pathways, two have been identified as thermodynamically and kinetically favorable reactions. These are (1) $CF_3CHFCF_3 \rightarrow CF_3CF{=}CF_2 + HF$, a four-center HF elimination pathway, and (2) $CF_3CHFCF_3 \rightarrow CF_3CHF + CF_3$, a C−C bond fission pathway. The best estimate of the $\Delta H_{r,298}$ for these processes are 34.8 and 92.3 kcal/mol using QCISD(T)/6-311G-(d,p)//UMP2/6-31G(d) methods, respectively. The barrier for $CF_3CHFCF_3 \rightarrow CF_3CF{=}CF_2 + HF$ was found to be 79.5 kcal/mol using the same methods. These results are discussed in light of past and current laboratory studies.

I. Introduction

One of the most common and most effective fire suppression agents used in the past was CF_3Br (Halon 1301). More recently, the Montreal Protocol has banned the production of Halon 1301 because of its contributions to stratospheric ozone depletion. Perhaps the most widely accepted replacement for Halon 1301 is 2-H heptafluoropropane (HFP). It has come into widespread[1] use in fire suppressant systems in most industrialized nations. HFP is also being considered for use as a propellant for drug administration. The fate of HFP after human inhalation has been studied by Aigbirhio and Pike.[2]

HFP suppresses flames by both chemical and physical mechanisms. HFP is able to extinguish flames physically by removing thermal energy from the flame. It is thought that HFP suppresses flames chemically by removing important species that are necessary for flame propagation.[3] Despite its widespread acceptance, the primary thermal decomposition behavior of (HFP) is still unclear. There have been several recent studies that have attempted to deduce the chemical behavior of HFP in high-temperature conditions.

Hynes et al.[4] studied the oxidation of HFP in a hydrogen−air flame. A detailed chemical kinetic mechanism was developed based both on previous studies[5,6] and on measured flame speed data. The mechanism of Hynes et al.[4] was based on three basic submechanisms: The GRI-Mech[5] for hydrogen and hydrocarbon oxidation, a hydrofluorcarbon reaction mechanism,[6] and their own HFP oxidation mechanism developed based on their experimental and modeling results. An interesting aspect of this study showed that stable CF_3CHFCF_3 may be formed through the addition of H to CF_3CFCF_3 and that CF_3CHFCF_3 decomposes primarily to form $CF_3CF{=}CF_2$ and HF or to form CF_3-CHF and CF_3. The study concluded that inhibition was accomplished in large part through reactions of H atoms with fluorinated species. These reactions produced less reactive molecules such as HF and several other radical species. A series of 42 reactions and their Arrhenius parameters were determined.

In the more recent study performed by Hynes et al.,[7] a shock tube study was used to propose three primary decomposition pathways. Reaction products were analyzed using GC−MS and FTIR techniques. In descending thermodynamic favorability, they are $CF_3CHFCF_3 \rightarrow CF_3CHF + CF_3$; $CF_3CHFCF_3 + F \rightarrow CF_3CFCF_3 + HF$; and $CF_3CHFCF_3 \rightarrow CF_3CF{=}CF_2 + HF$. A number of other thermal decomposition products were explained by proposed reactions involving the products of the three primary reaction pathways listed above. This study also discussed the reaction rates of the primary and secondary decomposition reactions.

Another recent study performed by Williams et al.[8] showed the behavior of HFP in a methane/oxygen flame. The composition of the HFP inhibited flame was analyzed to understand the chemical role of HFP in fire suppression. The primary initial decomposition pathways of HFP proposed in this study are CF_3-$CHFCF_3 \rightarrow CF_3CHF + CF_3$ and $CF_3CHFCF_3 \rightarrow CF_3CF{=}CF_2 + HF$. This study also focused on the kinetics of the above-mentioned reactions as well as a series of secondary reaction pathways. The kinetic mechanisms used in this study were adopted and modified from earlier studies done by NIST.[9]

Yamamoto et al.[10] performed an experiment to determine the temperature at which HFP decomposes, and the decomposition products were studied using GC/MS. Yamamoto et al.[10] found that HFP began to decompose at 500 °C, and it was nearly completely decomposed at temperatures of 700 °C and had disappeared at 800 °C. The main decomposition product was perfluoroisobutane.

In the present work, all bond fission and molecular pathways for the thermal decompositions are examined using ab initio and density functional theory calculations and are done to aid in understanding the origin of the reaction products observed by both Hynes et al.[4,7] and Williams et al.[8] In this study, we consider primary decomposition pathways. Some secondary reaction pathways, i.e., subsequent reaction decomposition channels after the initial decomposition steps are also examined to help interpret previous experiments in the literature.

II. Computational Methods

Ab initio molecular orbital calculations and density functional theory calculations were undertaken using Gaussian 98.[11] Geometry and frequency optimizations were performed using

10.1021/jp012763u CCC: $22.00
Published on Web 03/07/2002

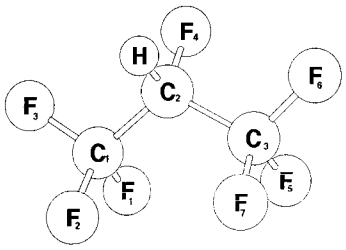

Figure 1. Geometry of 2-H Heptafluoropropane.

TABLE 1: Proposed 2-H Heptafluoropropane Degradation Pathways

reaction 1A	$CF_3CHFCF_3 \rightarrow CF_3CHF + CF_3$
reaction 1B	$CF_3CHF \rightarrow CF_2{=}CHF + F$
reaction 2	$CF_3CHFCF_3 \rightarrow CF_3CF_3 + CHF$
reaction 3	$CF_3CHFCF_3 \rightarrow CF_3CH{=}CF_2 + F_2$
reaction 4	$CF_3CHFCF_3 \rightarrow CF_3CF{=}CF_2 + HF$
reaction 5	$CF_3CHFCF_3 \rightarrow CF_3CHFCF + F_2$
reaction 6:	$CF_3CHFCF_3 \rightarrow CF_3CCF_3 + HF$
reaction 7	$CF_3CHFCF_3 \rightarrow CF_3CFCF_3 + H$
reaction 8	$CF_3CHFCF_3 \rightarrow CF_3CHCF_3 + F$
reaction 9	$CF_3CHFCF_3 \rightarrow CF_3CHFCF_2 + F$
reaction 10	$CF_3CHFCF_3 \rightarrow CF_3CH + CF_4$
reaction 11	$CF_3CHFCF_3 \rightarrow CF_3CF + CF_3H$
reaction 12	$CF_3CHFCF_3 \rightarrow CF_3CF_2H + CF_2$

B3LYP (Becke three-parameter hybrid functional combined with Lee, Yang, and Parr correlation functions)[12] and UMP2 (restricted and unrestricted second-order Møller−Plesset perturbation)[13] methodology at the 6-31G(d) basis set. The Berny analytical optimization routines[14,15] were used for molecular optimization. The density matrix was converged to 10^{-9} hartree, the threshold maximum displacement was 0.0018 Å, and the threshold of maximum force was 0.000 45 hartree/b. The transition-state molecules were characterized with the use of normal-mode analysis. The harmonic vibrational frequency was analyzed to ensure that the stable minimum of all positive frequencies were optimized and that transition-state frequency optimizations showed one imaginary frequency. The reaction coordinate of each molecule was also characterized to ensure that the true transition-state molecule was found. To improve the accuracy of the energetics, subsequent single-point calculations were performed using the UMP2/6-31G(d) optimized geometries. The single-point methodologies employed in this work were PMP4 (spin projected fourth-order Møller-Plesset perturbation theory, MP4SDTQ, frozen core)[16] and QCISD(T) (quadratic configuration interaction with single and double excitation incorporating the perturbative corrections for triple excitations)[17] at the 6-31G(d) and 6-311G(d,p) basis sets.

III. Results and Discussion

A. Optimized Structures and Vibrational Frequencies of HFP and Transition States. Figure 1 is a model of HFP based on the structure obtained from the UMP2/6-31G(d) optimization. The optimized geometry of HFP at both the B3LYP/6-31G(d) and UMP2/6-31G(d) levels of theory is listed in Table 2a. As seen in the table, both optimizations are in reasonably good agreement with each other. HFP belongs to the C_s point group. The backbone of the molecule is formed by a chain of three carbon atoms. Most carbon−fluorine bond lengths are approximately 1.34 Å, and each of the carbon centers shows a relatively predictable tetrahedral conformation. These results were seen in both the B3LYP/6-31G(d) and UMP2/6-31G(d) geometry optimizations. The three carbon atoms, which form the backbone of the molecule, form a slightly wide angle. Our B3LYP/6-31G(d) shows that this angle is 114.5°, and our UMP2/6-31G(d) optimization found that it is 114.3°.

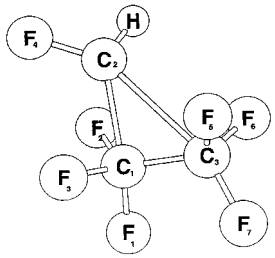

Figure 2. $CF_3CHFCF_3 \rightarrow CF_3CF_3 + CHF$ transition state.

The infrared spectrum of HFP has been previously studied. The spectrum was initially studied by Baker and Pulay,[18] who used HF and B3PW91 theoretical methodology to make infrared predictions. The gas phase FTIR spectrum of HFP was studied experimentally by McNaughton and Evans.[19] The results of our frequency optimizations of HFP are shown in Table 3 and may be compared to the experimental findings of McNaughton and Evans[19] and the theoretical findings of Baker and Pulay.[16] Our predictions match the observations and predictions of both comparative studies reasonable well. Our predicted relative peak intensities also correspond well with the studies performed by McNaughton and Evans and with the study performed by Baker and Pulay. In the study performed by McNaughton and Evans, peaks and band types were assigned. The zero-point vibrational energies for HFP using B3lYP/6-31G(d) and UMP2/6-31G(d) methods were found to be 31.6 and 32.4 kcal/mol, respectively. The thermal correction energies for HFP using B3lYP/6-31G(d) and UMP2/6-31G(d) methods were found to be 37.1 and 37.8 kcal/mol, respectively.

Reaction 2 ($CF_3CHFCF_3 \rightarrow CF_3CF_3 + CHF$) is the reverse reaction of the insertion of CHF into the C−C bond of CF_3-CF_3. Figure 2 shows our UMP2/6-31G(d) optimization of this transition-state molecule. The bonds joining the three carbon atoms both extend, although one extends much more than the other. Our UMP2/6-31G(d) optimization shows these bonds [$r(C_1C_2)$ and $r(C_2C_3)$] to be 1.97 and 2.56 Å. Carbon atoms one and three begin to get closer together as the molecule begins to resemble CF_3CF_3. The distance between the terminal carbon atoms (carbon atoms one and three) is 1.55 Å according to our best geometry optimization. The fluorine atoms connected to the terminal carbon atoms are oriented away from the leaving CHF molecule and form a nearly eclipsed conformation.

The transition state is characterized by one imaginary frequency of magnitude 726i at the UMP2/6-31G(d) level of theory, as shown in Table 4. The reaction coordinate of the transition state for reaction 2 is a complex mode principally involving hydrogen, the central and third carbon atom (carbon atoms two and three), and fluorine atom two. Hydrogen exhibits the greatest movement in this mode. The bond connecting it to carbon atom three bends such that hydrogen moves toward carbon atom one. Fluorine atom two oscillates in the direction of the central carbon atom (carbon atom two). This motion causes a twisting motion in the molecule.

Reaction 4 ($CF_3CHFCF_3 \rightarrow CF_3CF{=}CF_2 + HF$) is the 1,2 elimination reaction of HF from HFP. Figure 3 shows our optimized structure of the transition-state molecule for reaction 4 based on our UMP2/6-31G(d) results. In this four-center transition state, the CF [$r(C_3F_5)$] and CH [$r(C_2H)$] bonds stretch to 1.88 and 1.47 Å, respectively. The bond distance of HF [$r(HF_5)$] stretches to 1.162 Å. The UMP2/6-31G(d) optimization also shows shorter bond lengths between the carbon atoms involved in the transition state. The CC bond [$r(C_2C_3)$]

TABLE 2: B3LYP/6-31G(d) and UMP2/6-31G(d) Geometry Optimizations of 2-H Heptafluorpropane and Transition-State Molecules, in Angstroms and Degrees

	HFP		$[CF_3CF_3 + CHF]^‡$		$[CF_3CH{=}CF_2 + HF]^‡$		$[CF_3CCF_3 + HF]^‡$		$[CF_3CH + CF_4]^‡$		$[CF_3CF + CF_3H]^‡$		$[CF_3CF_2H + CF_2]^‡$	
coordinate	B3LYP/	UMP2/	B3LYP/	UMP2/	B3LYP/	UMP2/	B3LYP/	UMP2/	B3LYP/	UMP2/	B3LYP/	UMP2/	B3LYP/	UMP2/
$r(C_2C_1)$	1.533	1.519	2.040	1.970	1.506	1.493	1.506	1.500	1.494	1.487	1.531	1.527	1.543	1.534
$r(C_3C_2)$	1.533	1.519	2.612	2.560	1.434	1.424	1.506	1.500	2.103	2.044	2.363	2.325	2.018	1.936
$r(F_1C_1)$	1.339	1.339	1.362	1.381	1.341	1.341	1.353	1.349	1.352	1.351	1.347	1.347	1.339	1.342
$r(F_2C_1)$	1.345	1.345	1.638	1.586	1.352	1.353	1.345	1.346	1.349	1.349	1.348	1.349	1.340	1.343
$r(F_3C_1)$	1.343	1.344	1.324	1.333	1.348	1.348	1.347	1.347	1.358	1.358	1.342	1.342	1.344	1.342
$r(F_4C_2)$	1.374	1.379	1.322	1.325	1.373	1.378	1.909	1.795	1.641	1.620	1.332	1.338	1.364	1.391
$r(HC_2)$	1.095	1.093	1.101	1.098	1.410	1.436	1.856	1.631	1.092	1.091	1.213	1.233	1.085	1.086
$r(F_5C_3)$	1.340	1.339	1.332	1.335	1.921	1.882	1.353	1.349	1.309	1.314	1.326	1.326	1.702	1.696
$r(F_6C_3)$	1.343	1.344	1.341	1.345	1.294	1.297	1.347	1.347	1.312	1.317	1.336	1.337	1.315	1.315
$r(F_7C_3)$	1.345	1.345	1.343	1.340	1.291	1.294	1.345	1.346	1.337	1.347	1.327	1.328	1.322	1.322
$\theta(C_3C_2C_1)$	114.5	114.3	36.6	37.2	118.9	118.5	115.1	114.9	124.4	123.9	96.7	94.5	93.7	94.2
$\theta(C_1C_1C_2)$	111.9	111.7	145.9	148.5	110.2	110.3	104.5	105.6	106.8	107.1	107.2	106.5	111.4	110.4
$\theta(F_2C_1C_2)$	110.2	110.2	55.1	56.9	112.5	112.5	110.9	110.8	112.9	112.7	114.8	115.0	110.8	111.0
$\theta(F_3C_1C_2)$	109.3	109.2	93.4	92.9	110.2	110.2	117.4	116.2	114.5	114.2	109.7	110.0	109.5	110.4
$\theta(F_4C_2C_3)$	108.0	107.4	141.6	142.6	112.1	111.8	97.8	98.7	50.9	50.8	96.0	95.1	144.2	146.3
$\theta(HC_2C_3)$	108.2	108.8	109.6	108.6	78.1	77.2	112.0	114.2	120.7	121.3	28.1	26.7	88.6	90.5
$\theta(F_5C_3C_2)$	112.0	111.8	82.2	82.5	87.1	88.4	104.5	105.6	93.2	93.7	96.0	94.9	54.0	53.6
$\theta(F_6C_3C_2)$	109.3	109.2	82.1	81.9	123.4	123.1	117.4	116.2	92.5	92.8	120.0	120.4	130.0	129.5
$\theta(F_7C_3C_2)$	110.1	110.2	161.3	161.1	120.9	120.8	110.9	110.8	142.0	143.2	109.2	109.5	118.6	119.1
$\tau(F_1C_1C_2C_3)$	60.4	59.0	120.0	121.9	168.6	170.4	77.7	74.5	−136.5	−136.1	−175.4	−172.2	63.5	65.1
$\tau(F_2C_1C_2C_3)$	−60.7	−62.1	132.6	128.0	−71.6	−69.9	−165.3	−167.8	−17.5	−16.9	−55.9	−52.8	−58.5	−56.0
$\tau(F_3C_1C_2C_3)$	−179.7	178.8	−141.8	−115.2	48.5	50.2	−42.4	−45.9	104.3	104.4	66.6	70.0	−176.8	−174.9
$\tau(F_4C_3F_6F_7)$	−148.0	−149.4	164.8	163.5	135.0	132.9	85.9	87.1	100.0	99.8	160.2	162.0	−141.6	−142.1
$\tau(HC_3F_5F_6)$	−121.5	−119.5	60.2	59.4	119.6	119.6	149.9	148.0	87.3	87.5	108.0	109.4	159.2	158.4
$\tau(F_5C_1F_1F_2)$	−92.8	−94.3	146.9	145.7	157.0	156.4	150.4	150.3	67.1	66.7	71.3	64.6	−115.1	−115.4
$\tau(F_6C_1F_1F_3)$	137.7	137.5	−154.2	−154.0	−73.6	−74.3	−67.5	−67.1	−139.7	−139.3	−107.1	−115.9	170.7	172.9
$\tau(F_7C_1F_2F_3)$	−146.7	−148.3	−177.8	−176.3	103.5	103.9	116.3	116.6	103.6	103.4	56.8	56.6	−150.1	−149.4

TABLE 3: HFP Infrared Spectrum (cm^{-1})

	infrared absorbance bands					rel. intensities			
mode no.	B3LYP/ 6-31G(d)	UMP2/ 6-31G(d)	HF/ 6-311G(d,p)[a]	B3PW91/ 6-31(d)[a]	expt.[b]	B3LYP/ 6-31G(d)	UMP2/ 6-31G(d)	HF/ 6-311G(d,p)[a]	expt. strength[b]
1	3112.0	3174.2	2956	2985	2986.6	7.1	3.3	5.5	v. weak
2	1422.2	1476.1	1423	1389	1395.4	98.2	141.0	165	medium
3	1406.4	1441.1	1390	1371	1399.9	5.8	16.0	20	medium
4	1329.4	1370.3	1319	1310	1309.3	288.5	280.3	455	strong
5	1298.6	1345.4	1288	1277	1283.7	91.8	43.0	65	medium
6	1272.7	1307.9	1269	1248	1247.4	261.4	286.0	436	strong
7	1245.7	1278.5	1237	1221	1223.2	322.5	304.7	280	strong
8	1207.2	1244.3	1214	1183	1189.0	16.7	23.6	26	weak
9	1151.0	1177.6	1143	1129	1128.4	79.3	183.2	256	strong
10	1148.4	1170.2	1132	1120	1128.4	189.9	67.1	130	strong
11	914.5	936.6	899	891	908.8	41.3	50.3	61	medium
12	871.8	895.3	853	855	862.7	33.5	35.2	39	weak
13	736.4	745.7	735	737	742.8	14.6	14.3	22	weak
14	678.1	686.3	681	693	689.9	47.7	48.8	70	medium
15	603.1	615.1	599	597	612	0.3	0.5	1.5	v. weak
16	542.5	550.9	545	541	552	1.4	1.8	2.1	v. weak
17	526.7	533.0	530	526	535	3.9	4.7	7.0	weak
18	508.9	516.9	513	516	516	9.1	10.9	17	weak
19	449.2	457.1	449	458	454.4	2.3	2.7	3.7	v. weak
20	339.6	346.9	339	347	-	0.1	0.1	0.0	-
21	321.9	331.2	317	323	323.8	0.5	0.5	1.2	v. weak
22	288.6	293.9	287	297	392.1	0.3	0.4	0.8	v. weak
23	234.2	238.1	238	238	242	1.9	2.1	2.5	v. weak
24	222.0	228.7	216	215	226	3.5	3.9	5.7	weak
25	162.0	167.4	151	158	150.7	1.3	1.4	2.2	v. weak
26	90.9	101.9	87	84	-	0.2	0.2	0.2	
27	16.8	27.0	26	18	-	0.0	0.0	0.0	

[a] Theoretical study performed by Baker and Pulay. [b] Experimental study performed by McNaughton and Evans.

connecting these two carbon atoms narrows to 1.42 Å. The bond angles of the atoms on the two carbon centers involved in the transition state become more trigonal planar in nature.

The reaction coordinate exhibited by this transition state involves the hydrogen atom and its movement with respect to the $CF_3CF{=}CF_2$ group. This vibrational band is one in which hydrogen oscillates between fluorine atom four and carbon atom one. This is a complex mode, and as the hydrogen stretches away from carbon atom four, carbon atom two stretches toward carbon atom one.

Reaction 6 ($CF_3CHFCF_3 \rightarrow CF_3CCF_3 + HF$) is a 1,1 HF elimination reaction involving a three center transition state. Figure 4 shows our optimized structure of the transition state. In this transition state, the bonds between the central carbon

TABLE 4: UMP2/6-31G(d) Frequency Optimizations for 2-H Heptafluoropropane Reaction Products and Transition States

Products		
species	vibrational frequency (cm-1)	ZPE (kcal/mol)
CF_3CHF	3303 1504 1341 1255 1228 1212 886 719 674 557 517 421 352 213 87	20.4
CF_3CHF	1318 1317 1126 704 504 504	7.8
CF_2CHF	3336 1870 1417 1317 1202 951 771 621 559 482 311 225	18.7
CF_3CHFCF_3CHF	1505 1308 1308 1293 1293 1153 815 707 622 622 517 517 380 354 214 67	19.0
CHF	2884 1482 1261	8.0
$CF_3CHFCHCF_2$	3311 1849 1457 1358 1332 1227 1173 993 895 824 713 640 597 583 531 419 383 327 193 137 10	27.1
F_2	1008	1.4
$CF_3CHFCFCF_2$	1877 1466 1388 1274 1250 1241 1060 772 654 641 604 558 509 465 372 363 249 242 182 122 36	21.9
HF	4042	5.8
$CF_3CHFCHFCF$	3109 1409 1354 1327 1284 1238 1189 1181 1001 844 686 617 547 515 463 373 275 232 192 133 54	25.8
$CF_3CHFCCF_3CHF$	1403 1353 1316 1246 1182 1145 939 841 706 656 555 537 520 499 333 285 231 165 84 75	20.6
$CF_3CHFCFCF_3CHF$	1466 1447 1316 1268 1257 1224 1211 1011 792 709 701 662 550 536 503 458 349 329 295 251 174 136 52 25	23.9
$CF_3CHFCHCF_3CHF$	3334 1498 1375 1301 1291 1241 1203 1158 936 886 772 659 635 543 538 518 464 334 309 299 220 141 41 31	28.1
$CF_3CHFCHFCF_2$	3179 1478 1428 1375 1353 1310 1261 1190 1115 949 903 769 711 595 552 520 410 343 304 229 214 153 84 37	29.3
CF_3CHFCH	3104 1388 1312 1160 1090 857 599 558 530 514 339 240	16.7
CF4	1344 1344 1344 918 628 628 628 432 432	11.0
CF_3CHFCF	1364 1287 1282 1241 852 697 542 530 409 363 278 16	12.7
CF_3CHFH	3237 1465 1465 1219 1172 703 505 505	16.4
CF_3CHFCF_2H	3193 1516 1443 1373 1284 1252 1200 1172 898 728 589 575 518 418 365 246 210 78	24.4
CF_2	1281 1180 667	4.5

Transition States		
reaction	vibrational frequency (cm^{-1})	ZPE (kcal/mol)
rxn 2	3115 1414 1396 1299 1279 1246 1217 1117 997 858 751 662 609 568 552 521 468 397 370 337 317 249 185 149 95 66 726i	28.9
rxn 4	1772 1614 1478 1413 1273 1249 1224 1137 1039 816 789 722 621 604 551 503 432 380 351 291 274 247 199 166 78 54 1883i	27.6
rxn 6	1328 1404 3139 1295 1262 1223 1212 962 860 736 678 678 596 546 527 518 507 344 319 302 286 205 171 155 95 29 777i	27.7
rxn 10	3210 1394 1381 1324 1235 1209 1170 1055 934 890 771 703 659 616 589 558 527 496 434 342 318 248 200 108 84 51 749i	29.3
rxn 11	2121 1446 1349 1311 1284 1262 1223 1211 1036 870 807 699 665 564 521 519 515 430 282 254 245 195 185 128 81 52 1383i	27.6
rxn 12	1979 1767 1395 1330 1273 1230 1183 1178 1110 947 890 733 695 588 560 538 512 453 349 330 271 235 195 124 83 56 874i	28.6

and the hydrogen and fluorine [$r(C_2H)$ and $r(C_2F_4)$] attached to it extent beyond what is observed in HFP to 1.63 and 1.78 Å, respectively. Our UMP2/6-31G(d) optimization showed these same bonds in the HFP molecule to be 1.09 and 1.38 Å, respectively. The angle between these atoms becomes a very shallow 33.4°. The distance between hydrogen and fluorine [$r(HF_4)$] becomes 1.00 Å. As these two atoms extend away from their original carbon center, the distances between the carbon atoms becomes shorter. The CC bonds between both become 1.50 Å. Comparatively, the HFP bond lengths were 1.52 and 1.51 Å.

The reaction coordinate seen in the transition state for reaction 6 principally involves the movement of the hydrogen atom. In this vibrational mode, hydrogen maintains its distance from carbon atom one and fluorine atom three as it rotates toward the plane formed by fluorine atom three, carbon atom one, and carbon atom four.

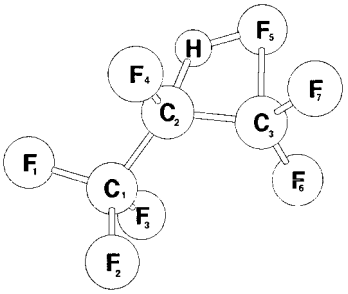

Figure 3. $CF_3CHFCF_3 \rightarrow CF_3CF{=}CF_2 + HF$ transition state.

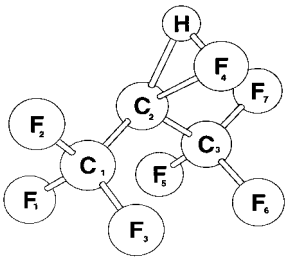

Figure 4. $CF_3CHFCF_3 \rightarrow CF_3CCF_3 + HF$ transition state.

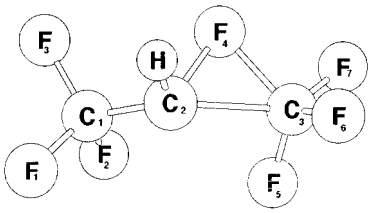

Figure 5. $CF_3CHFCF_3 \rightarrow CF_3CH + CF_4$ transition state.

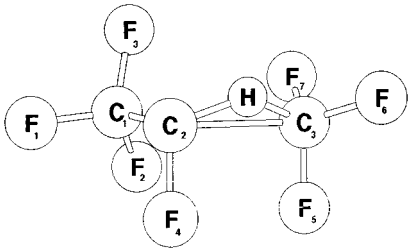

Figure 6. $CF_3CHFCF_3 \rightarrow CF_3CF + CF_3H$ transition state.

Reaction 10 ($CF_3CHFCF_3 \rightarrow CF_3CH + CF_4$) is a three-center fluorine atom transfer reaction. Figure 5 shows a model of the UMP2/6-31G(d) findings for this transition state. The primary changes we see to the molecular geometry include an extension of the bond connecting the carbon atoms involved in the transition state [$r(C_2C_3)$] and the extension of the bond between the central fluorine atom and the central carbon atom [$r(C_2F_4)$]. The distance between carbon atoms involved in the transition becomes 2.04 Å. The bond between the central fluorine atom (F_4) and the central carbon atom (C_2) is 1.62 Å. The change in distance between the carbon atoms involved in the transition state [$r(C_2C_3)$] indicates that the molecule is beginning to dissociate. This combined with the fact that the central fluorine atom (F_4) begins to stretch away from and the central carbon atom (C_2) and bend toward the third carbon atom shows how the CF_4 group is formed.

The reaction coordinate of reaction 10 mainly involves carbon atoms one and two, hydrogen, and fluorine atom three. The bond joining hydrogen and the central carbon atom (C_2) stretches symmetrically away from the leaving CF_4 group.

Reaction 11 ($CF_3CHFCF_3 \rightarrow CF_3CF + CF_3H$) is a three-center hydrogen atom transfer reaction. Figure 6 is a model of this transition state developed based on our UMP2/6-31G(d) geometry optimization. The geometry of this transition state is analogous to the transition state for reaction 10. The main difference between the two molecules is that in reaction 11 we see the hydrogen atom migrating toward the leaving carbon atom (C_3) and its attached fluorine atoms. The hydrogen atom extends away from the central carbon atom in this transition to a distance of 1.23 Å. The distance between the hydrogen and the leaving CF_3 group is 1.34 Å. Similar to the reaction 10 transition state, the bond distance between the carbon atoms involved in the transition state [$r(C_2C_3)$] elongates to 2.33 Å

The reaction coordinate of the transition state of reaction 11 shows the movement of hydrogen in the direction of the leaving carbon atom (C_3). This mode is indicative of the migration of hydrogen toward the CF_3 group.

Reaction 12 ($CF_3CHFCF_3 \rightarrow CF_3CF_2H + CF_2$) is the reverse reaction of the insertion of CF_2 into the CF bond of CF_3CF_2H. The transition state is a three-center reaction and is depicted in Figure 7 based on our UMP2/6-31G(d) geometry optimization. Evidence of this transition state lies in several of the geometric parameters involving the migrating fluorine atom (F_5) and the carbon atoms involved in the transition state (C_2 and C_3). The distance between the central carbon atom (C_2) and the fluorine

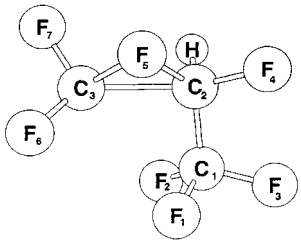

Figure 7. $CF_3CHFCF_3 \rightarrow CF_3CF_2H + CF_2$ transition state.

atom that is transferred to the CF_3CF_2H (F_5) is 1.65 Å, whereas its distance from the leaving CF_2 group is 1.70 Å according to our UMP2/6-31G(d) geometry optimization. Another important characteristic of the transition state for reaction 12 is the distance between the carbon atoms involved in the transition state (C_2 and C_3). Our UMP2/6-31G(d) geometry optimization shows this distance is 1.936 Å, whereas in HFP, this distance is 1.519 Å. The fluorine atoms of the CF_2 group (F_6 and F_7) also form slightly shorter bonds with carbon (C_3); they are 1.32 Å. These distances in HFP are 1.34 and 1.35 Å, respectively.

The reaction coordinate of the reaction 12 transition state mainly involves the stretching of the bonds which join the atoms that make up the three-center portion of the transition state. The carbon atoms involved in the transition state (C_2 and C_3) and the migrating fluorine atom (F_5) stretch symmetrically as the molecule prepares to dissociate.

B. Energetics of HFP Decomposition Pathways. The total energies for all reactants, products, and transition states are given in the Supplementary Information (Table 8). The enthalpy of reaction for the specific decomposition pathways is presented in Table 5. Also included are the enthalpies of reaction obtained using the respective single-point methodology: PMP4/6-31G(d), QCISD(T)/6-31G(d), PMP4/6-311G(d,p), and QCISD(T)/6-311G(d,p). All single-point calculations were performed using the optimized structural parameters obtained in the above listed UMP2/6-31G(d) geometry optimization. Table 6 gives a complete list of the transition-state energy barriers. Single-point energies listed in Tables 5 and 6 were scaled to 0 and 298 K using UMP2/6-31G(d) optimized zero-point vibrational energies and thermal correction energies, respectively.

Examination of the $\Delta H_{r,298}$ for the various methodologies used in this study shows an interesting trend in differences of results (see Figure 8. Root mean square differences between results obtained using B3LYP/6-31G(d) methods and UMP2/6-31G(d), PMP4/6-31G(d), and QCISD(T)/6-31G(d) methods were of 6.2, 3.6, and 3.2 kcal/mol, respectively. Comparison of the results obtained by UMP2/6-31G(d) with PMP4/6-31G(d) and QCISD(T)/6-31G(d) results showed larger RMS differences of 5.2 and 6.7 kcal/mol, respectively. RMS differences between PMP4 and QCISD(T) at the 6-31G(d) and 6-311G(d) basis sets tended to be quite low. With the 6-31G(d) basis set, the RMS difference between results obtained using PMP4 and QCISD(T) methods was 1.8 kcal/mol, and with the 6-311G(d) basis set, this difference was 1.6 kcal/mol. Slightly greater RMS differences exist between different basis set predictions obtained using the PMP4 or QCISD(T) methodologies. The RMS difference between the results obtained using PMP4 methods at the 6-31G(d) and 6-311G(d) basis sets is 4.9 kcal/mol. The RMS difference between the results obtained using these basis sets combined with QCISD(T) methodology is 4.5 kcal/mol. The RMS differences show that the QCISD(T) methodology with the 6-311G(d,p) basis set show the smallest root mean square errors associated with the results.

Reaction 1A shows the decomposition of HFP to form CF_3CHF and CF_3 and is suggested by Hynes et al.[7] as one of the

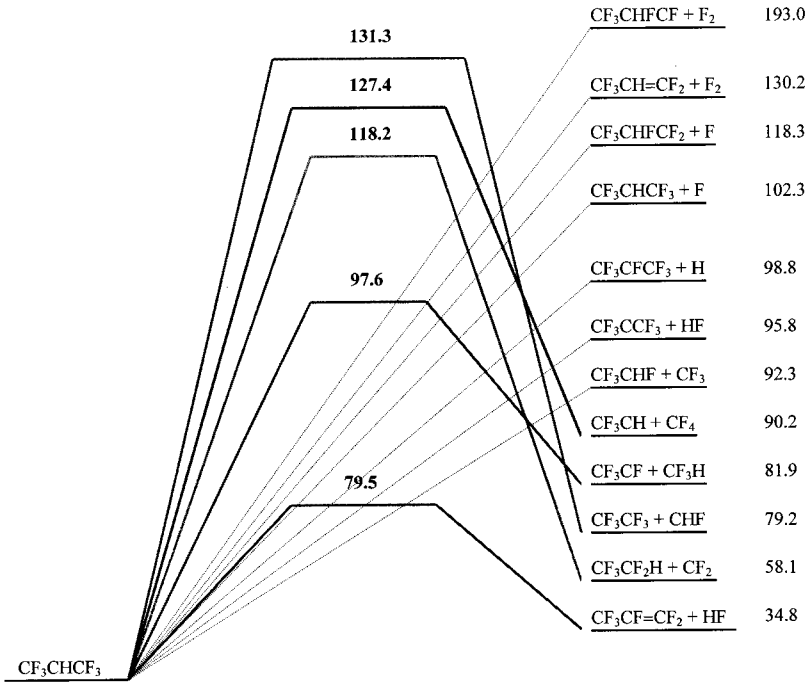

Figure 8. Energy diagram of CF_3CHFCF_3 primary decomposition pathways.

TABLE 5: Enthalpy of Decomposition Reactions for 2-H Hepthafluoropropane at 0 K (kcal/mol)

	6-31G(d)				6-311G(d,p)		
	B3LYP/	UMP2/	PMP4/	QCISD(T)/	PMP4/	QCISD(T)/	QCISD(T)[a]
rxn 1A	88.3	98.6	100.7	98.9	98.2	96.3	92.3
rxn 1B	69.5	70.4	67.3	67.1	62.6	64.2	61.8
rxn 2	85.8	92.6	92.6	91.2	89.7	88.2	79.2
rxn 3	128.6	137.0	136.5	134.5	134.9	133.6	130.2
rxn 4	43.2	45.2	49.7	49.1	38.9	38.5	34.8
rxn 5	194.2	205.9	201.2	198.2	200.1	197.5	193.0
rxn 6	105.2	109.9	111.7	109.2	103.1	100.7	95.8
rxn 7	96.9	93.9	102.2	102.2	107.2	107.2	98.8
rxn 8	106.6	110.6	108.8	107.6	106.0	106.7	102.3
rxn 9	122.4	128.8	125.6	124.4	121.3	121.7	118.3
rxn 10	92.4	100.2	100.6	97.6	97.8	95.0	90.2
rxn 11	83.7	92.1	89.7	88.2	86.6	85.1	81.9
rxn 12	60.9	66.5	64.7	64.1	62.1	61.4	58.1[a]

[a] At 298 K.

TABLE 6: Barrier Heights of Decomposition Reactions of 2-H Heptafluoropropane at 0 K (kcal/mol)

	6-31G(d)				6-311G(d,p)		
	B3LYP/	UMP2/	PMP4/	QCISD(T)/	PMP4/	QCISD(T)/	QCISD(T)[a]
rxn 2	123.2	133.7	131.6	133.3	133.0	134.6	131.3
rxn 4	75.4	83.2	87.4	89.1	82.3	84.2	79.5
rxn 6	90.3	95.9	97.7	97.1	93.4	92.9	88.7
rxn 10	118.9	128.3	127.6	128.6	129.3	130.4	127.4
rxn 11	95.6	108.1	107.6	107.2	102.3	102.0	97.6
rxn 12	108.8	119.2	117.6	119.5	119.1	121.0	118.2

most likely HFP decomposition initiation mechanisms. The experimental findings of Hynes et al.[7] combined with the computational work of Chen et al.[20] provide a $\Delta H_{r,298}$ value of 87.8 kcal/mol (367 kJ/mol) for this initiation reaction. Our QCISD(T)/6-311G(d,p) single-point calculation yielded a comparable $\Delta H_{r,298}$ of 92.3 kcal/mol (386.2 kJ/mol). This reaction mechanism is thought to be one of the most important initiation reactions because its products could further react to form products observed in the experiment. For example, reaction 1B shows the decomposition of CF_3CHF to form CF_2═CHF and F. Large amounts of CF_2═CHF were detected by both Hynes et al.[7] and Williams et al.[8] Hynes' experimental $\Delta H_{r,298}$ for this reaction is 62.1 kcal/mol (260 kJ/mol), whereas results showed a $\Delta H_{r,298}$ of 61.8 kcal/mol (258.6 kJ/mol). In the experimental and kinetic modeling study performed by Williams et al.,[8] the kinetic parameter for this reaction was revised. The corrected parameters predicted this C−C bond rupture mechanism as the predominating HFP removal mechanism.

Although the decomposition of HFP to form CF_3CHF and CF_3 is thought to be one of the more important initiation mechanisms, the decomposition of HFP to form C_3F_6 and HF is thermodynamically more feasible. Of our list of proposed decomposition pathways, reactions 4 and 6 show the formation of C_3F_6 isomers and HF. In reaction 4, we see the decomposition of HFP to form CF_3CF═CF_2 and HF. Reaction 6 shows the formation of CF_3CCF_3 and HF. In the study of Hynes et al.,[7]

we see that the $\Delta H_{r,298}$ for the formation of C_3F_6 and HF is 129 kJ/mol. Reactions 4 and 6 of this study differ both in reaction energies as well as in transition-state energies. Our QCISD(T)/6-311G(d,p) calculation shows a $\Delta H_{r,298}$ of 34.8 kcal/mol (145.6 kJ/mol) for reaction 4 and 95.8 kcal/mol (400.8 kJ/mol) for reaction 6. The barrier height of reaction 4 was also lower than that of reaction 6; they were 79.5 (332.6) and 88.7 kcal/mol (371.1 kJ/mol), respectively. This is important considering that from Hynes et al.[7] we learn that the most prevalent HFP decomposition product is C_3F_6.

Trace amounts of CF_3CF_2H were also observed by Hynes et al.[4] In their study, they propose that CF_3CF_2H is formed by CHF_2 and CF_3 bonding. Our study considers the possibility that CF_3CF_2H may be formed through reaction 12 in which HFP decomposes to form CF_3CF_2H and CF_2, both of which were detected in the study performed by Hynes et al.[7] The $\Delta H_{r,298}$ for reaction for reaction 12 is 58.1 kcal/mol (243.1 kJ/mol) according to our QCISD(T)/6-311G(d,p) findings. Although reaction 12 showed one of the lowest reaction enthalpy of all of the listed reactions, it showed a comparatively high activation energy barrier. This could account for why only small amounts of CF_3CF_2H were found in the study performed by Hynes et al.[7]

In the study performed by Williams et al.,[8] CF_2 is formed via a different channel than that of Hynes et al.[7] Hynes et al.[7] propose that destruction of $CF_2{=}CF_2$ yields two molecules of CF_2. Williams shows that CF_2 may originate from CF_3 reactions with hydrogen, which form CF_2 and HF. It may also be a result of the reaction of $CHF{=}CF_2$ with hydrogen atoms, which yields CH_2F and CF_2. Another noted product detected by Hynes et al.[7] is C_2F_4 which may have several origins. Hynes et al.[7] suggest that C_2F_4 may arise from the C−C bond fission of C_3F_6 to form CF_3CF and CF_2. Their reaction enthalpy at 298 K was experimentally determined to be 78.4 kcal/mol (328 kJ/mol). Findings of the present work shows that CF_2 may form via reaction 12 ($CF_3CHFCF_3 \rightarrow CF_3CF_2H + CF_2$) which has a $\Delta H_{r,298}$ of 58.1 kcal/mol (243.1 kJ/mol) and a predicted barrier height of 118.2 kcal/mol (494.5 kJ/mol) according to our QCISD(T)/6-311G(d,p) results. In reaction 11, we consider the possibility that HFP may decompose to form CF_3CF and CF_3H. The results of our QCISD(T)/6-311G(d,p) study show a $\Delta H_{r,298}$ for reaction 11 of 81.9 kcal/mol (342.7 kJ/mol), and the predicted activation energy was 97.6 kcal/mol (408.4 kJ/mol). CF_3CF is an important molecule because it may lead to the formation of the C_2F_4. The isomerization reaction was found by DiFelice and Ritter[21] to be −75.3 kJ/mol.

Hynes et al.[6,7] propose that the most likely pathway for the formation of CF_3CF_3 is through the recombination of CF_3 radicals, which form in reaction 1. CF_3CF_3 is one of the more common decomposition products of HFP. This study shows that CF_3CF_3 may form through the path described in reaction 2 in which HFP decomposes to form CF_3CF_3 and CHF. Our QCISD-(T)/6-311G(d,p) calculations show a moderately high $\Delta H_{r,298}$ (79.2 and 331.4 kJ/mol) for this reaction. The activation energy barrier was also rather high (131.3 and 549.4 kJ/mol). On the basis of our findings, reaction 2 would not be the dominant HFP decomposition pathway but may explain the origin of some of the HFP decomposition products observed by Hynes et al. On the basis of our data, the CF_3 radical combination reaction which yields CF_3CF_3 $\Delta H_{r,298}$ is 99.1 kcal/mol (414.6 kJ/mol).

The reaction enthalpy and barrier height results for several of the reactions studied in this work suggest that they are slower or less likely to proceed than many of the others. Reaction 3 ($CF_3CHFCF_3 \rightarrow CF_3CH{=}CF_2 + F_2$) is similar to reaction 4, and it seems plausible that HFP may also undergo this decomposition. In reaction 3 we see that HFP decomposes to form $CF_3CH{=}CF_2$ and F_2. The $\Delta H_{r,298}$ for this reaction was much higher than many of the others (130.2 and 544.6 kJ/mol) as compared to 34.8 kcal/mol (145.6 kJ/mol) for reaction 4. The 298 K reaction enthalpy of reaction 10 ($CF_3CHFCF_3 \rightarrow CF_3CH + CF_4$) is 90.2 kcal/mol (377.5 kJ/mol), and the barrier height (at 298 K) is 127.4 kcal/mol (532.9 kJ/mol) according to our QCISD(T)/6-311G(d,p) findings. Despite this, reaction 10 should be considered because of the products that are formed. Hynes et al.[7] note that small amounts of CF_4 were detected in runs where the temperature exceeded 1550 K. The formation of CF_4 is explained by Hynes et al.[7] in their experimental work through the reaction of CF_3 and an F atom. Our data allows easy calculation of the 298 K enthalpy of this reaction; it is 123.8 kcal/mol (518.0 kJ/mol) according to our QCISD(T)/6-311G(d,p) findings. Discussion of the presence of CF_3CH was not found in our literature search.

Reactions 7−9 also showed relatively low $\Delta H_{r,298}$ values. Reaction 7 involves HFP decomposition to form CF_3CFCF_3 and one hydrogen atom. Reaction 8 is analogous to reaction 7 in that HFP decomposes to form CF_3CHCF_3 and one fluorine atom. According to our QCISD(T)/6-311G(d,p) calculation the $\Delta H_{r,298}$ for reaction 8 is 102.3 kcal/mol (427.8 kJ/mol), whereas for reaction 7, it is 98.8 kcal/mol (413.2 kJ/mol). Reaction 9 involves the dissociation of one fluorine atom from carbon atom three. The products of this reaction are CF_3CHFCF_2 and one fluorine atom. According to our QCISD(T)/6-311G(d,p) calculation $\Delta H_{r,298}$ for this reaction is 118.3 kcal/mol (494.8 kJ/mol); thus, this reaction is higher in energy than both reactions 7 or 8. The only reaction higher in energy was reaction 5 in which HFP decomposes to form CF_3CHFCF and F_2. According to our QCISD(T)/6-311G(d,p) calculation, the $\Delta H_{r,298}$ for this reaction is 193.0 kcal/mol (807.3 kJ/mol) and the most thermodynamically unlikely of all of the studied reactions.

This study considers new decomposition pathways of HFP which may have previously been overlooked. Many of the molecules formed in our proposed reaction pathways were detected in the studies of Hynes et al.[4,7] and further studied by Williams et al.[8] The molecules that appear in their studies most frequently were HF, CF_3, CF_2, F, $CHFCF_2$, and $CHFCF_3$. According to the results of our study, HF may form through either reaction 4 or 6. Reaction 6 was not previously considered as a possible channel for HF formation, and it is not as thermodynamically feasible as is reaction 4. These molecules may be explained more simply by considering several of the reaction pathways undertaken in this study. Reaction 1A ($CF_3CHFCF_3 \rightarrow CF_3 + CF_3CHF$) is a reaction pathway that has already been considered in the work of both Hynes et al.[7] and Williams et al.[8] The origin of CF_2 appears in the work of Hynes et al.[7] quite frequently as secondary reaction products. This study proposes that CF_2 may be formed through the decomposition of HFP to form CF_2 and CF_3CF_2H (reaction 12). This reaction was also one of the more thermodynamically feasible reaction pathways of this study. The formation of CHF was also not previously considered to be a primary decomposition product of HFP in either previous studies.[7,8] Reaction 2 of this study considers the possibility that CHF may be a result of HFP decomposition. Reaction 1B shows that CF_3CHF may decompose to form CF_2CHF and one fluorine atom. Reaction 1B also explains the origin of CF_2CHF, one of the products detected in the study performed by Hynes et al.[7] Hynes et al.[7] use a total of 68 reaction paths to explain HFP decomposition products, whereas Williams et al.[8] use a slightly simplified version

including 23 reaction pathways. Results from the present study suggest that the decomposition reaction model by both Hynes et al.[7] and Williams et al.[8] could be further simplified.

IV. Conclusion

In this study, we have performed accurate calculations which have allowed us to investigate several HFP decomposition pathways previously not taken into account. We have located the transition-state molecules for several of the reactions of this study and described the geometries and vibrational frequencies of the molecules. The energetic characteristics of these molecules have helped us understand the relative importance of these reactions. According to past experimental studies, HFP decomposition has been limited to two or three main initiation steps, followed by a long list of secondary reactions to explain the origin of the observed products. This study shows how HFP decomposes in ways that were not previously considered and provides new insight into the behavior of HFP in high-temperature environments. These results should help explain the origin of several decomposition products. Moreover, our results suggest that there may be little need for complex secondary reaction schemes to describe the thermal decomposition mechanism of HFP.

Supporting Information Available: Tables S1-S8 showing data from the experiments. This material is available free of chrge via the Internet at http://pubs.acs.org.

References and Notes

(1) Miziolek, A. W., Tsang, W., Eds.; *Halon Replacements: Technology and Science*; ACS Symposium Series 611; American Chemical Society: Washington, DC, 1994.

(2) Aigbirhio, F. I.; Pike, V. W. *J. Fluorine Chem.* **1995**, *75*, 67.

(3) Robin, M. L. Fire Protection in Telecommunication Facilities. *Process Saf. Prog.* **2000**, *19, 2*, 107.

(4) Hynes, R. G.; Mackie, J. C.; Masri, A. R. *Combust. Flame* **1998**, *113*, 554.

(5) Frenklach, M.; Wang, H.; Goldenberg, M.; Smith, G. P.; Golden, D. M.; Bowman, C. T.; Hanson, R. K.; Gardiner, W. C.; Lissianski, V. *GRI-mech: An Optimized Detailed Chemical Reaction Mechanism for Methane Combustion*; Report No. GRI-95/0058, 1995; http://www.me.berkeley.edu/gri_mech/.

(6) Burgess, D. R., Jr.; Zachariah, M. R.; Tsang, W.; Westmoreland, P. R. *Prog. Energy Combust. Sci.* **1996**, *21*, 453.

(7) Hynes, R. G.; Mackie, J. C.; Masri, A. R. *J.Phys. Chem. A* **1999**, *103*, 54.

(8) Williams, B. A.; L'Esperance, D. M.; Fleming, J. W. *Combust. Flame* **2000**, *120*, 160.

(9) The U.S. National Institute of Standards and Technology mechanisms can be found at http://www.fluid.nist.gov/.

(10) Yamamoto, T.; Yasuhara, A.; Shiraishi, F.; Kaya, K.; Abe, T. *Chemosphere* **1997**, *35*−*3*, 643.

(11) Frisch, M. J.; Trucks, G. W.; Schlegel, H. B.; Scuseria, G. E.; Robb, M. A.; Cheeseman, J. R.; Zakrzewski, V. G.; Montgomery, J. A., Jr.; Stratmann, R. E.; Burant, J. C.; Dapprich, S.; Millam, J. M.; Daniels, A. D.; Kudin, K. N.; Strain, M. C.; Farkas, O.; Tomasi, J.; Barone, V.; Cossi, M.; Cammi, R.; Mennucci, B.; Pomelli, C.; Adamo, C.; Clifford, S.; Ochterski, J.; Petersson, G. A.; Ayala, P. Y.; Cui, Q.; Morokuma, K.; Malick, D. K.; Rabuck, A. D.; Raghavachari, K.; Foresman, J. B.; Cioslowski, J.; Ortiz, J. V.; Stefanov, B. B.; Liu, G.; Liashenko, A.; Piskorz, P.; Komaromi, I.; Gomperts, R.; Martin, R. L.; Fox, D. J.; Keith, T.; Al-Laham, M. A.; Peng, C. Y.; Nanayakkara, A.; Gonzalez, C.; Challacombe, M.; Gill, P. M. W.; Johnson, B. G.; Chen, W.; Wong, M. W.; Andres, J. L.; Head-Gordon, M.; Replogle, E. S.; Pople, J. A. *Gaussian 98*, revision A.7; Gaussian, Inc.: Pittsburgh, PA, 1998.

(12) Becke, A. M. *J. Chem. Phys.* **1993**, *98*, 5648.

(13) Pople, J. A.; Krushnan, R.; Schlegel, H. B.; Binkley, J. S. *Int. J. Quantum Chem. Quantum Chem. Symp.* **1979**, *13*, 225.

(14) Schlegel, H. B. *J. Comput. Chem.* **1982**, *3*, 214.

(15) Schlegel, H. B. *J. Chem. Phys.* **1982**, *77*, 3676.

(16) Krishnan, R.; Pople, J. A. *Int. J. Quantum Chem.* **1978**, *14*, 91.

(17) Pople, J. A.; Head-Gordon, M.; Raghavachari, K. *J. Chem. Phys.* **1987**, *87*, 5968.

(18) Baker, J.; Pulay, P. *J. Comput. Chem.* **1998**, *19*, 1187.

(19) McNaughton, D.; Evans, C. J. *Spectrochim. Acta A* **1999**, *55*, 1177.

(20) Chen, Y.; Rauk, A.; Tschuikow-Roux, E. *J. Chem. Phys.* **1991**, *94*, 7299.

(21) DiFelice, J.; Ritter, E. R. *Combust. Sci. Technol.* **1996**, *5*, 116.